CHAPTER XX-3

THE "VIRTUAL DENTITION" OF THE SPY VI CHILD

Priscilla BAYLE & Roberto MACCHIARELLI

Abstract

Spy VI is a recently recognised Neandertal immature individual from the cave of Betche aux Rotches, Belgium (Rougier et al.*, 2004). It is represented by four isolated deciduous teeth associated with two mandibular fragments (Crevecoeur* et al.*, this volume: chapter XX-2). In detail, the teeth consist of an upper right and a lower left central incisors (Spy 589a and 592a, respectively), a lower right lateral incisor (Spy 594a), and a lower left canine (Spy 645a). We investigated this new dental fossil material by means of advanced techniques of µCT-based 3D virtual rendering and subtle quantitative structural analysis.*

With the only exception of the deciduous lower canine, the values of the total tooth volume displayed by Spy VI fit the estimates available for the Neandertal child of Roc de Marsal (MIS 5a, France) and largely exceed the modern human figures. In dental tissue proportions, while the Spy VI whole amount of tooth crown enamel is comparable to the modern condition, the dentine volume is systematically larger, a pattern typical of Neandertal teeth. Another typical feature shared by all four Spy VI teeth is represented by the huge dimensions of their pulp cavities.

INTRODUCTION

Differences in linear enamel thickness and pulp cavity dimensions have been traditionally used to characterise the Neandertal dental structural condition with respect to the modern human one in terms of ontogeny, palaeobiology, dietary habits, and palaeoenvironmental constraints (Adloff, 1907; Gorjanović-Kramberger, 1907, 1908; Keith & Knowles, 1911; Keith, 1913; Legoux, 1966; Trinkaus, 1983; Tillier *et al.*, 1989; Zilberman *et al.*, 1992; Zilberman & Smith, 1992; Molnar *et al.*, 1993; Smith & Zilberman, 1994; Ramirez Rozzi, 1996; Grine, 2004). Most of the observations leading to these interpretations rely on radiographic-based bidimensional (2D) estimates. The increasing use in palaeoanthropology of microtomographic investigative techniques (µCT, SR-µCT) allowing the noninvasive, high-resolution 3D modelling and quantitative characterisation of the fossil dental record discloses new perspectives in this research domain (e.g. Kono, 2004; Mazurier & Macchiarelli, 2005; Olejniczak & Grine, 2005; Macchiarelli *et al.*, 2006, 2007, 2008; Smith *et al.*, 2007a, 2007b, 2010; Bayle, 2008a, 2008b; Olejniczak *et al.*, 2008; Bayle *et al.*, 2009a, 2009b, 2010).

With special reference to the permanent molars, results from this new generation of microstructural studies show that Neandertals differ from modern humans, notably in volumetric dental tissue proportions (Macchiarelli *et al.*, 2006, 2008; Olejniczak *et al.*, 2008). While the total amount of enamel is comparable, the Neandertal enamel-dentine junction (EDJ) is more complex and the dentine volume larger than the modern one (Macchiarelli *et al.*, 2006; Skinner *et al.*, 2008). Consequently, Neandertal enamel is distributed over a larger dentine surface, thus resulting in lower average enamel thickness values (Olejniczak *et al.*, 2008).

While preliminary observations on deciduous dental elements confirm these observations (in Bayle, 2008a), it is noteworthy that only a few Upper Pleistocene specimens have been described so far for the inner structure of their primary dentition, notably of the anterior arcade teeth (Mazurier & Macchiarelli, 2005; Macchiarelli *et al.*, 2006, 2007; Bayle, 2008a, 2008b; Bayle *et al.*, 2009a, 2009b, 2010; Toussaint *et al.*, 2010; Benazzi *et al.*, 2011).

The re-evaluation of the odontoskeletal Neandertal collection from the cave of Betche aux

Rotches, near Spy, Belgium (Fraipont & Lohest, 1886, 1887), allowed the identification of the previously unrecognised remains of an immature individual, labelled Spy VI (Rougier *et al.*, 2004), represented by four isolated deciduous teeth associated with two mandibular fragments (Crevecoeur *et al.*, this volume: chapter XX-2). In detail, the specimens represent: an upper right and a lower left central incisors (Spy 589a and 592a, respectively), a lower right lateral incisor (Spy 594a), and a lower left canine (Spy 645a). Based on extant maturational reference standards, the Spy VI dental developmental stage points to an age-at-death of 16 ± 6 months (Crevecoeur *et al.*, 2010, this volume: chapter XX-2).

Here, we report the results from the "virtual" investigation of this newly discovered dental material from Spy generated by means of advanced techniques of µCT-based 3D rendering and subtle quantitative structural analysis. More specifically, for each dental element, we assessed the linear, surface, and volumetric proportions of its crown and root components (enamel, dentine, pulp), and also detailed the global and topographic enamel thickness variation, as well as the tooth-specific enamel/dentine ratio. Finally, despite the still meagre deciduous comparative record available for this set of virtual dental variables (see *infra*), we compared these results to the figures from the 2.5-3.0-year-old Neandertal child of Roc de Marsal, Dordogne, France (Bayle, 2008b; Bayle *et al.*, 2009b), and to a recent modern reference sample (Bayle, 2008a, 2008b).

METHODS

The four isolated teeth of Spy VI have been detailed in 2005 by using a SkyScan 1076 *in vivo* microtomograph set at the Micro CT Scan Research Group laboratory of the University of Antwerp (Belgium). Scans were realised according to the following parameters: 100 kV, 100 µA current, 16 integrations/projection, and a projection each 0.7°. The final volume was reconstructed with an isotropic voxel size of 17.69 μm^3 using the software NRecon v.1.3 (SkyScan). In order to facilitate processing procedures, the resolution was halved, thus leading to a voxel size of 35.38 μm^3.

A semi-automatic segmentation with manual corrections was carried out by means of AMIRA v.4.1.2 (Mercury Computer Systems, Inc.) and Artecore v.1.0 (NESPOS Society). Threshold values between segmented components were found according to the methodology developed by Spoor & co-workers (1993), taking repeated measurements on different slices of the virtual stack (Coleman & Colbert, 2007). For individual measurements, crowns were digitally isolated from roots (Olejniczak *et al.*, 2008) and surface rendering was performed using triangulation and constrained smoothing from the volumetric data (marching cube algorithm; Lorensen & Cline, 1987).

The following 12 linear, surface, and volumetric variables describing tooth tissue proportions were digitally measured or calculated: Vt = total tooth volume (mm^3); Ve = volume of the enamel cap (mm^3); Vd = total volume of the dentine (mm^3); Vp = total volume of the pulp (mm^3); Vcdp = volume of the coronal dentine (including the coronal aspect of the pulp chamber) (mm^3); Vcd = volume of the coronal dentine (excluding the coronal aspect of the pulp chamber) (mm^3); Vcp = volume of the coronal pulp (mm^3); Vc = total volume of the crown (mm^3); Vcdp/Vc = percent of coronal volume that is dentine and pulp; Sedj = surface area of the enamel-dentine junction (mm^2); AET = average enamel thickness (mm); and RET = scale-free relative enamel thickness (for methodological details, see Kono, 2004; Macchiarelli *et al.*, 2006; Olejniczak *et al.*, 2008).

For each crown, the 3D mapping of the enamel thickness topographic distribution was realised from the segmented enamel and crown dentine components by means of AMIRA v.4.1.2 (Mercury Computer Systems, Inc.). The relative site-specific thickness variation has been rendered by using a chromatic scale (thickness increasing from dark blue up to red; for methodological details, see Macchiarelli *et al.*, 2007, 2008).

Intra- and inter-observer tests for accuracy of the measures were run by two observers (P.B. and an independent trained observer). As a whole, recorded differences are less than 5 %,

which is compatible with previous results on similar sets of 2-3D virtually assessed variables (e.g. Kono, 2004; Suwa & Kono, 2005; Olejniczak & Grine, 2006).

In the comparative analysis, beside the record from the MIS 5a Neandertal child from Roc de Marsal (Bayle *et al.*, 2009b), the recent human condition (RMH) is represented by the average values calculated from five selected individuals of European origin aged 1.5-4 years, whose unworn deciduous lower dentition has been detailed by means of the same µCT analytical procedures (Bayle, 2008a).

RESULTS AND DISCUSSION

The virtually reconstructed four deciduous teeth of Spy VI (Udi1 589a, Ldi1 592a, Ldi2 594a, and Ldc 645a) are distinctly shown in Figure 1 to Figure 4 (lingual aspect). For each

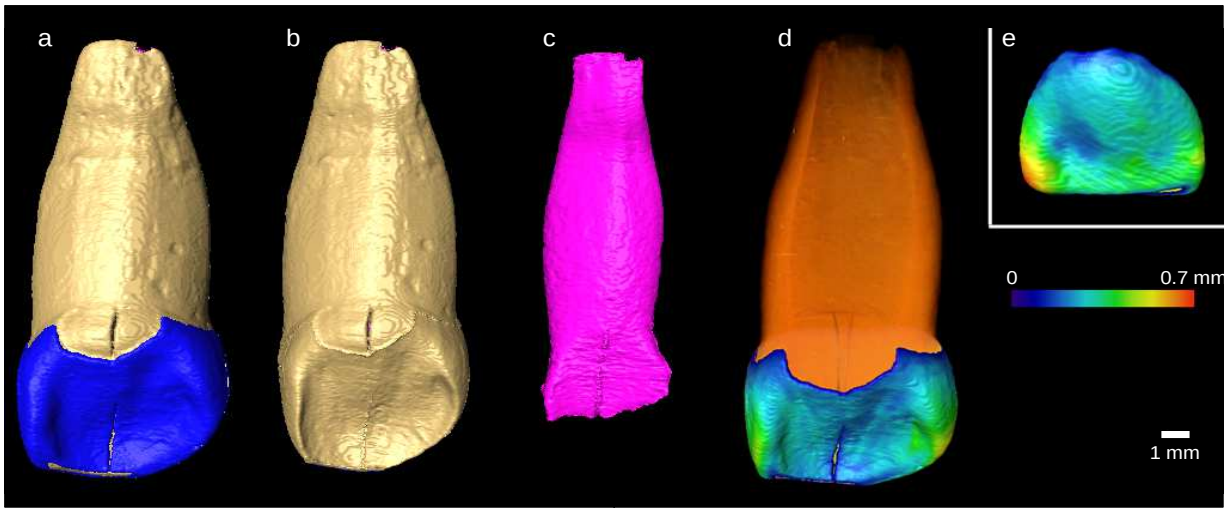

Figure 1. Virtual reconstruction and 3D rendering in lingual view of the Spy 589a upper right deciduous central incisor (Udi1). a: enamel (in blue) and dentine; b: dentine after enamel removal; c: virtual filling of the pulp cavity after removal of the surrounding tissues; d: enamel thickness topographic variation (stepped scale ranging from “thin” dark blue to “thick” red); e (inset): enamel thickness topographic variation in a same tooth-type recent human crown (scale code as in d).

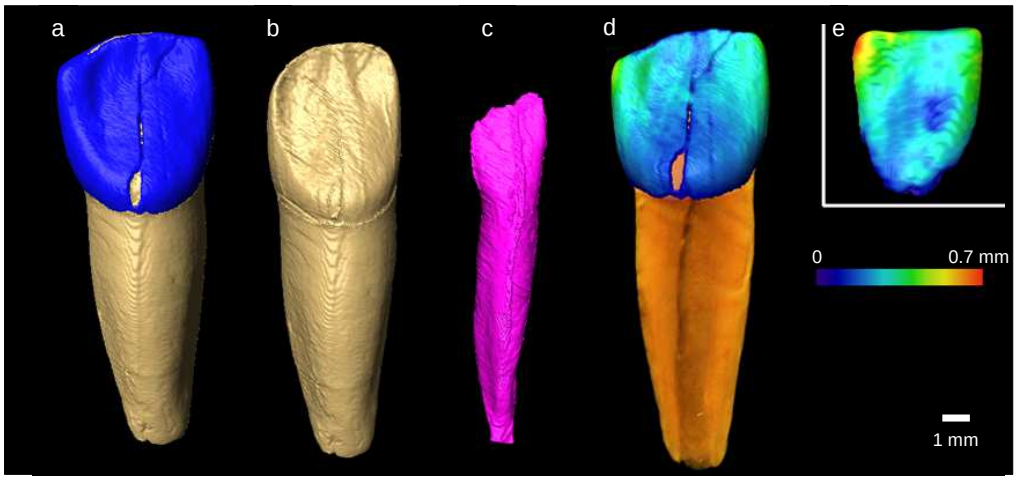

Figure 2. Virtual reconstruction and 3D rendering in lingual view of the Spy 592a lower left deciduous central incisor (Ldi1). a-e as in Figure 1.

tooth, the enamel (in blue) and the dentine (a), the dentine after enamel removal (b), the virtual filling of the pulp cavity after removal of the surrounding tissues (c), and the enamel thickness topographic variation (d; stepped scale) are rendered separately within each figure. The enamel thickness mapping assessed for the same tooth-type in a reference recent human crown (same view and stepped scale) is also provided for comparison (inset e in top right corner).

As described by the 12 linear, surface, and volumetric selected variables, comparative dental tissue proportions estimated for each tooth-type in Spy VI, Roc de Marsal 1 (RdM; Bayle, 2008a, 2008b; Bayle *et al.*, 2009b), and a recent human reference sample (RMH average values; Bayle, 2008a) are shown in Table 1.

With the only exception of the Spy 645a deciduous lower canine, the values displayed by

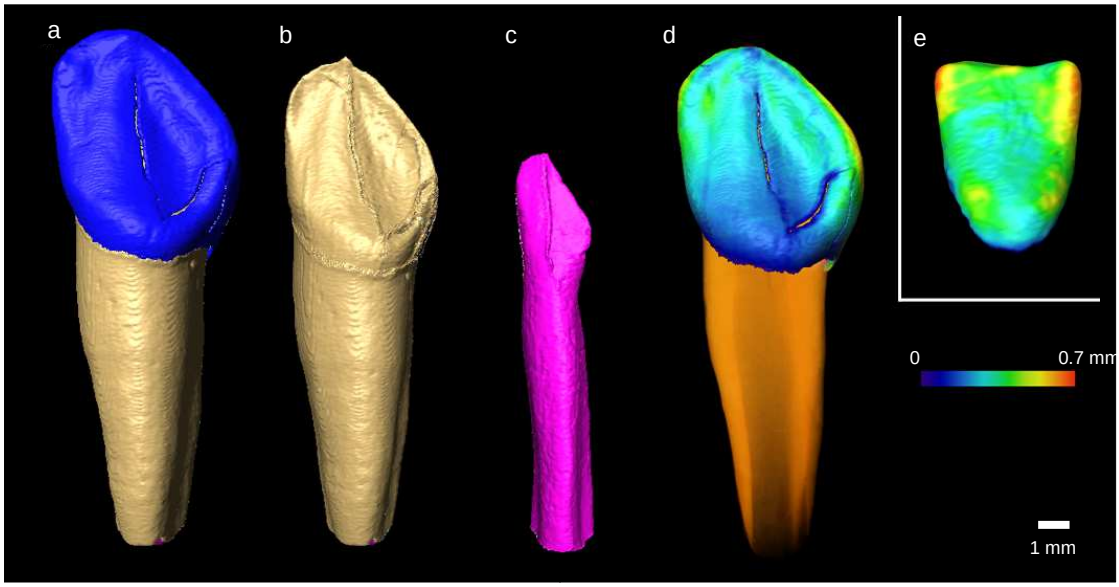

Figure 3. Virtual reconstruction and 3D rendering in lingual view of the Spy 594a lower right deciduous lateral incisor (Ldi2). a-e as in Figure 1.

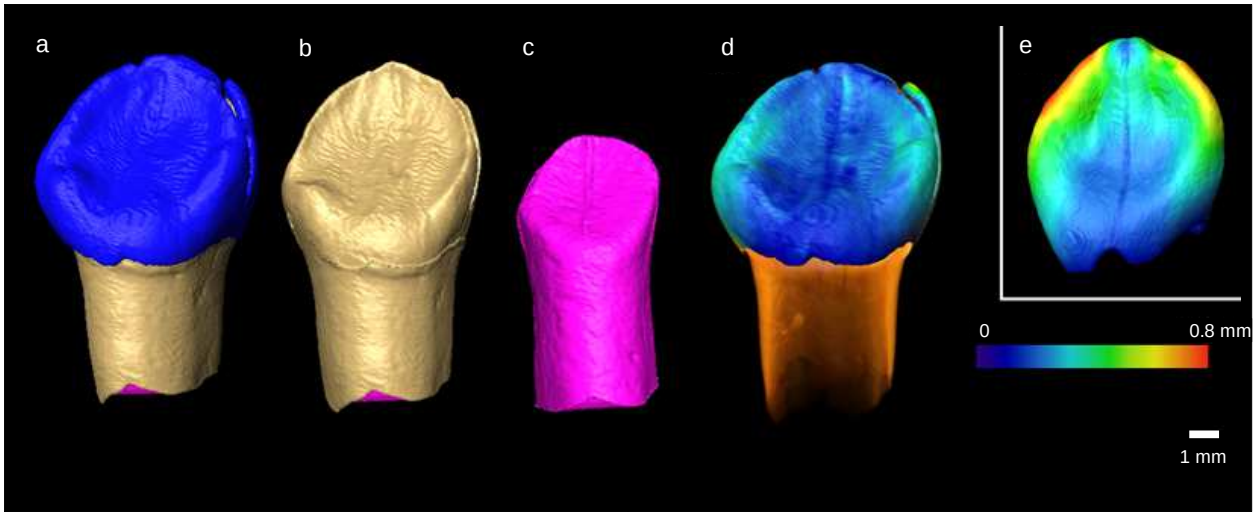

Figure 4. Virtual reconstruction and 3D rendering in lingual view of the Spy 645a lower left deciduous canine (Ldc). a-e as in Figure 1.

Spy VI for the total tooth volume (Vt) are close to (but more often higher than) the estimates of the Roc de Marsal child, and thus largely exceed the recent human condition. In this specific comparative context, beside the possible effect of diagenetic factors, the pattern shown by Spy 645a can be explained by its relatively lower maturational degree with respect to both RdM and the modern specimens. In fact, according to the descriptive criteria for the deciduous calcification stages set by Liversidge & Molleson (2004), while the Spy VI canine corresponds to stage "e" (where root formation is more than a spicule, but root length is less than crown height; Crevecoeur *et al.*, 2010), those of RdM and RMH fit stages "f" or "g" (rooth length from incomplete, but greater than crown height, to almost complete, with apical edges parallel or slightly converging).

As observed in other similar analyses performed on Neandertal teeth (Mazurier & Macchiarelli, 2005; Macchiarelli *et al.*, 2006, 2007; Bayle, 2008a, 2008b; Bayle *et al.*, 2009a, 2009b), differences in relative tissue proportions (volumes) between Spy VI and Roc de

		Vt (mm^3)	*Ve* (mm^3)	*Vd* (mm^3)	*Vp* (mm^3)	*Vcdp* (mm^3)	*Vcd* (mm^3)	*Vcp* (mm^3)	*Vc* (mm^3)	*Vcdp/Vc* (%)	*Sedj* (mm^2)	*AET* (mm)	*RET*
Udi1	Spy VI	275.01	26.59	186.94	61.48	87.27	76.05	11.22	113.86	77	93.21	0.29	6.43
	RdM[1]	283.33	30.24	204.40	48.69	96.76	83.32	13.44	127.01	76	92.67	0.33	7.11
	Spy VI / RdM	**0.97**	**0.88**	**0.91**	**1.26**	**0.90**	**0.91**	**0.83**	**0.90**	**1.01**	**1.01**	**0.87**	**0.90**
	Mean RMH[1]	178.15	26.15	130.54	21.46	51.69	46.02	5.67	77.84	66	68.05	0.38	10.32
	Spy VI / RMH	**1.54**	**1.02**	**1.43**	**2.87**	**1.69**	**1.65**	**1.98**	**1.46**	**1.15**	**1.37**	**0.74**	**0.62**
Ldi1	Spy VI	143.29	16.05	100.40	26.85	39.18	34.04	5.15	55.23	71	61.06	0.26	7.74
	RdM[1, 2, 3]	125.35	12.72	100.63	12.00	40.61	37.24	3.38	53.33	76	49.97	0.25	7.41
	Spy VI / RdM	**1.14**	**1.26**	**1.00**	**2.24**	**0.96**	**0.91**	**1.52**	**1.04**	**0.93**	**1.22**	**1.03**	**1.04**
	Mean RMH[1]	73.04	12.45	53.46	7.13	16.59	14.63	1.95	29.04	58	33.42	0.38	14.78
	Spy VI / RMH	**1.96**	**1.29**	**1.88**	**3.77**	**2.36**	**2.33**	**2.64**	**1.90**	**1.22**	**1.83**	**0.70**	**0.52**
Ldi2	Spy VI	175.10	20.91	111.83	42.36	44.55	40.27	4.28	65.46	68	63.92	0.33	9.23
	RdM[1, 2, 3]	159.01	18.49	123.04	17.48	44.47	40.55	3.92	62.96	71	62.55	0.30	8.34
	Spy VI / RdM	**1.10**	**1.13**	**0.91**	**2.42**	**1.00**	**0.99**	**1.09**	**1.04**	**0.96**	**1.02**	**1.11**	**1.11**
	Mean RMH[1]	94.66	18.58	65.23	10.85	21.06	18.65	2.42	39.65	53	43.77	0.43	15.68
	Spy VI / RMH	**1.85**	**1.13**	**1.71**	**3.90**	**2.11**	**2.16**	**1.77**	**1.65**	**1.27**	**1.46**	**0.76**	**0.59**
Ldc	Spy VI	166.28	25.52	68.08	72.68	76.87	49.79	27.08	102.39	75	85.51	0.30	7.02
	RdM[1, 2, 3]	281.37	33.16	187.56	60.65	79.57	70.35	9.22	112.73	71	88.19	0.38	8.74
	Spy VI / RdM	**0.59**	**0.77**	**0.36**	**1.20**	**0.97**	**0.71**	**2.94**	**0.91**	**1.06**	**0.97**	**0.79**	**0.80**
	Mean RMH[1]	186.05	32.49	122.55	31.01	48.51	44.25	4.26	81.00	60	65.23	0.50	13.84
	Spy VI / RMH	**0.89**	**0.79**	**0.56**	**2.34**	**1.58**	**1.13**	**6.35**	**1.26**	**1.25**	**1.31**	**0.60**	**0.51**

Table 1. Virtually assessed linear, surface, and volumetric estimates and dental tissue proportions of the Spy VI deciduous teeth (Udi1, Ldi1, Ldi2, Ldc) compared to those of the Neandertal child from Roc de Marsal (Bayle, 2008a, 2008b; Bayle *et al.*, 2009b) and to the average values calculated from five recent individuals (RMH; Bayle, 2008a). Vt = total tooth volume (mm^3); Ve = volume of the enamel cap (mm^3); Vd = total volume of the dentine (mm^3); Vp = total volume of the pulp (mm^3); Vcdp = volume of the coronal dentine (including the coronal aspect of the pulp chamber) (mm^3); Vcd = volume of the coronal dentine (excluding the coronal aspect of the pulp chamber) (mm^3); Vcp = volume of the coronal pulp (mm^3); Vc = total volume of the crown (mm^3); Vcdp/Vc = percent of coronal volume that is dentine and pulp; Sedj = surface area of the enamel-dentine junction (mm^2); AET = average enamel thickness (mm); RET = scale-free relative enamel thickness. [1]Bayle, 2008a; [2]Bayle, 2008b; [3]Bayle *et al.*, 2009b.

Marsal 1, on one side, and the modern human condition represented by the comparative sample included in this study (RMH) are not homogeneously distributed among enamel, dentine, and pulp. In fact, while the indicators of average (AET) and relative (RET) enamel thickness systematically show thinner Neandertal enamel, the absolute volumes (Ve) are similar (Table 1).

The comparative enamel thickness cartographies shown in Figure 1 to Figure 4 (d *vs*. inset e) clearly illustrate the extent of the differences between Spy VI and a recent human counterpart. While global distribution patterns overlap (relatively thinner and thicker areas tend to correspond), site-specific quantitative differences in enamel thickness distribution are evident.

Conversely, except for the still incompletely developed Spy 645a lower canine, dentine (Vd) and pulp volumes (Vp) are significantly larger in Spy VI and RdM (for estimates on permanent Neandertal molars, see Macchiarelli *et al.*, 2006, 2008; Olejniczak *et al.*, 2008; Bayle *et al.*, 2009b, 2010; Toussaint *et al.*, 2010; Benazzi *et al.*, 2011). In Table 1, this pattern can be clearly observed by comparing the estimates of the percent of coronal volume that is dentine and pulp (Vcdp/Vc), the values ranging from 68 % to 77 % in the two Neandertal individuals and from 53 % to 66 % in the comparative modern sample.

Even in respect to the child of Roc de Marsal, the most remarkable feature displayed by the Spy VI teeth is likely represented by the generalised huge dimensions of their pulp cavities (Vp and Vcp in Table 1; see also c and d in Figure 1 to Figure 4), which are clearly reminiscent of the high degree of taurodontism traditionally reported in Neandertal decidous and permanent cheek teeth (Keith, 1913; Blumberg *et al.*, 1971; Mena, 1971; Grine & Klein, 1985; Constant & Grine, 2001). With special regard to the Neandertal primary dentition, while this condition had been already described for the molars (e.g. Zilberman *et al.*, 1992; Smith & Zilberman, 1994), to the best of our knowledge, it had not yet been reported for the front teeth (see Vallois, 1957 for a report on a permanent front tooth).

CONCLUDING REMARKS

The radiographic analysis of 25 Neandertal and 91 modern molar teeth performed by Zilberman & co-workers (1992) represents the most extensive study realised so far on deciduous dental tissue proportions of Upper Pleistocene and Holocene humans. Accordingly, with respect to the modern condition, Neandertals show comparable dentine heights, but lower enamel heights and widths, and greater enamel to floor of pulp chamber and pulp heights and widths (Zilberman *et al.*, 1992). Nonetheless, more recent 3D analyses show that a direct 2D comparison of enamel and dentine heights that does not take into account volumetric differences does not fully reflect tooth structural complexity (Macchiarelli *et al.*, 2006, 2007; Olejniczak *et al.*, 2008).

Present evidence from the Spy VI anterior "virtual dentition", as well as from the Roc de Marsal child (Bayle, 2008a, 2008b; Bayle *et al.*, 2009b) and other Neandertal front teeth (Mazurier & Macchiarelli, 2005; Macchiarelli *et al.*, 2007; Bayle, 2008a), fits the pattern described on larger quantitative ground for the deciduous and permanent Neandertal molars (Macchiarelli *et al.*, 2006, 2008; Bayle, 2008a, 2008b; Olejniczak *et al.*, 2008; Bayle *et al.*, 2009a, 2009b, 2010; Toussaint *et al.*, 2010; Benazzi *et al.*, 2011). As a whole, compared to modern teeth, both posterior and anterior Neandertal crowns are characterised by a bulky dentine associated to comparable enamel volumes.

Results from Spy VI also show the poorly known (or at least yet to be quantified; see Vallois, 1957) "taurodontic" morphology of the Neandertal anterior teeth, a structural feature which is in accordance with their proportionally large external linear measurements and global volume (e.g. Brace & Mahler, 1971; Frayer, 1978; Wolpoff, 1979; Trinkaus, 1983; Macchiarelli & Bondioli, 1986). The extension of this feature in the Neandertal dental record and its chrono-geographical variation range should deserve greater attention in the future.

Together with some differences in external crown and root morphology and general tooth size, since the first stages of their growth,

Neandertal teeth show an inner structural organisation which differs from that characteristic of anatomically modern humans (Bayle *et al.*, 2009a, 2010; Benazzi *et al.*, 2011). While direct/indirect relationships with a number of factors, such as specific developmental mechanisms and trajectories (e.g. Suwa & Kono, 2005; Macchiarelli *et al.*, 2006; Smith *et al.*, 2007b, 2010, 2011; Bayle, 2008a, 2008b; Bayle *et al.*, 2009a, 2009b), and/or, for example, ecological constraints or dietary specialisations (e.g. Richards *et al.*, 2001) are certainly possible, the adaptative nature of these differences awaits future research. In this perspective, it is likely that deciduous teeth will be major protagonists (Macchiarelli & Bailey, 2007).

ACKNOWLEDGEMENTS

We are sincerely indebted to the Editors for their kind invitation to contribute this unique volume and, mostly, for having put at disposition of the international scientific community the original record in their care. The French *Musée National de Préhistoire*, at Les Eyzies-de-Tayac, kindly granted access to the original skeleton of Roc de Marsal used for comparison with the fossil material from Spy (courtesy of J.-J. Cleyet-Merle). The UMR 5199 PACEA-LAPP, Bordeaux 1 Univ. (M. Bessou, B. Maureille, and P. Murail) and the *Institut d'Anatomie de Strasbourg* (J.-L. Kahn) provided comparative materials for high-resolution analyses. We acknowledge for technical collaboration the ESRF beamline ID17, Grenoble (A. Bravin and C. Nemoz) and the *Centre de Microtomographie* at the Univ. of Poitiers (A. Mazurier and P. Sardini). Special thanks for their substantial contribution to L. Bondioli, J. Braga, I. Crevecoeur, and A. Mazurier. Research supported by the EU FP6 Marie Curie Actions MRTN-CT-2005-019564 (EVAN), the Fyssen Foundation, the TNT and GDR 2152 CNRS projects, and the NESPOS Society (https:// www.nespos.org/display/openspace/Home).

BIBLIOGRAPHY

ADLOFF P., 1907. Die Zähne des *Homo primigenius* von Krapina. *Anatomischer Anzeiger*, **31**: 273-282.

BAYLE P., 2008a. *Analyse Quantitative par Imagerie à Haute Résolution des Séquences de Maturation Dentaire et des Proportions des Tissus des Dents Déciduales chez les Néanderthaliens et les Hommes Modernes*. Thèse de doctorat, Université Paul Sabatier, Toulouse.

BAYLE P., 2008b. Proportions des tissus des dents déciduales chez deux individus de Dordogne (France): l'enfant néanderthalien du Roc de Marsal et le spécimen du Paléolithique supérieur final de La Madeleine. *Bulletins et Mémoires de la Société d'Anthropologie de Paris*, **20** (3-4): 151-163.

BAYLE P., BRAGA J., MAZURIER A. & MACCHIARELLI R., 2009a. Brief communication: high-resolution assessment of the dental developmental pattern and characterization of tooth tissue proportions in the late Upper Paleolithic child from La Madeleine, France. *American Journal of Physical Anthropology*, **138** (4): 493-498.

BAYLE P., BRAGA J., MAZURIER A. & MACCHIARELLI R., 2009b. Dental developmental pattern of the Neanderthal child from Roc de Marsal: a high-resolution 3D analysis. *Journal of Human Evolution*, **56** (1): 66-75.

BAYLE P., MACCHIARELLI R., TRINKAUS E., DUARTE C., MAZURIER A. & ZILHÃO J., 2010. Dental maturational sequence and dental tissue proportions in the early Upper Paleolithic child from Abrigo do Lagar Velho, Portugal. *Proceedings of the National Academy of Sciences USA*, **107**: 1338-1342.

BENAZZI S., FORNAI C., BAYLE P., COQUERELLE M., KULLMER O., MALLEGNI F. & WEBER G. W., 2011. Comparison of dental measurement systems for taxonomic assignment of Neanderthal and modern human lower second deciduous molars. *Journal of Human Evolution*, **61**: 320-326.

BLUMBERG J. E., HYLANDER W. L. & GOEPP R. A., 1971. Taurodontism: a biometric study. *American Journal of Physical Anthropology*, **34** (2): 243-256.

BRACE C. L. & MAHLER P. E., 1971. Post-Pleistocene changes in the human dentition. *American Journal of Physical Anthropology*, **34** (2): 191-203.

COLEMAN M. N. & COLBERT M. W., 2007. Technical note: CT thresholding protocols for taking measurements on three-dimensional models. *American Journal of Physical Anthropology*, **133** (1): 723-725.

CONSTANT D. A. & GRINE F. E., 2001. A review of taurodontism with new data on indigenous southern African populations. *Archives of Oral Biology*, **46**: 1021-1029.

CREVECOEUR I., BAYLE P., ROUGIER H., MAUREILLE B., HIGHAM T., VAN DER PLICHT J., DE CLERCK N. & SEMAL P., 2010. The Spy VI child: a newly discovered Neandertal infant. *Journal of Human Evolution*, **59**: 641-656.

FRAIPONT J. & LOHEST M., 1886. La race humaine de Néanderthal ou de Canstadt, en Belgique. Recherches ethnologiques sur des ossements humains, découverts dans des dépôts quaternaires d'une grotte à Spy et détermination de leur âge géologique. Note préliminaire. *Bulletin de l'Académie royale des Sciences de Belgique*, 3ème série, **XII**: 741-784.

FRAIPONT J. & LOHEST M., 1887. La race humaine de Néanderthal ou de Canstadt en Belgique. Recherches ethnologiques sur des ossements humains, découverts dans des dépôts quaternaires d'une grotte à Spy et détermination de leur âge géologique. *Archives de Biologie*, **7**/1886: 587-757.

FRAYER D. W., 1978. *Evolution of the dentition in Upper Paleolithic and Mesolithic Europe*. Ph.D. Dissertation, University of Kansas, Lawrence: 201 p.

GORJANOVIĆ-KRAMBERGER D., 1907. Die Kronen und Wurzeln der Mahlzähne des *Homo primigenius* und ihre genetische Bedeutung. *Anatomischer Anzeiger*, **31**: 97-134.

GORJANOVIĆ-KRAMBERGER D., 1908. Über prismatische Molarwurzeln rezenter und diluvialer Menschen. *Anatomischer Anzeiger*, **32**: 401-413.

GRINE F. E., 2004. Geographic variation in human tooth enamel thickness does not support Neandertal involvement in the ancestry of modern Europeans. *South African Journal of Science*, **100**: 389-394.

GRINE F. E. & KLEIN R. G., 1985. Pleistocene and Holocene human remains from Equus Cave, South Africa. *Anthropology*, **8**: 55-97.

KEITH A., 1913. Problems relating to the teeth of the earlier forms of prehistorical man. *Proceedings of the Royal Society of Medicine*, **6**: 103-119.

KEITH A. & KNOWLES F., 1911. A description of teeth of Palaeolithic man from Jersey. *Journal of Anatomy and Physiology*, **46**: 12-27.

KONO R., 2004. Molar enamel thickness and distribution patterns in extant great apes and humans: new insights based on a 3-dimensional whole crown perspective. *Anthropological Science*, **112**: 121-146.

LEGOUX P., 1966. *Détermination de l'âge dentaire de fossiles de la lignée humaine*. Paris, Maloine S. A.: 307 p.

LIVERSIDGE H. M. & MOLLESON T., 2004. Variation in crown and root formation and eruption of human deciduous teeth. *American Journal of Physical Anthropology*, **123** (2): 172-180.

LORENSEN W. E. & CLINE H. E., 1987. Marching cubes: a high-resolution 3D surface construction algorithm. *Computer Graphics (ACM)*, **21**: 163-169.

MACCHIARELLI R. & BAILEY S. E., 2007. Dental microstructure and life history: introduction. *In*: S. E. BAILEY & J.-J. HUBLIN (ed.), *Dental Perspectives on Human Evolution. State-of-the-Art Research in Dental Paleoanthropology*. Dordrecht, Springer: 139-146.

MACCHIARELLI R. & BONDIOLI L., 1986. Morphometric changes in permanent dentition through the Neolithic: a microregional analysis. I. Upper dentition. *Homo*, **37**: 239-256.

MACCHIARELLI R., BONDIOLI L., DEBÉNATH A., MAZURIER A., TOURNEPICHE J.-F., BIRCH W. & DEAN C., 2006. How Neanderthal molar teeth grew. *Nature*, **444**: 748-751.

MACCHIARELLI R., BONDIOLI L. & MAZURIER A., 2008. Virtual dentitions: touching the hidden evidence. *In*: J. D. IRISH & G. C. NELSON (ed.), *Technique and application in dental anthropology*. Cambridge, Cambridge University Press: 426-448.

MACCHIARELLI R., MAZURIER A. & VOLPATO V., 2007. L'apport des nouvelles technologies à l'étude des Néandertaliens. *In*: B. VANDERMEERSCH & B. MAUREILLE (ed.), *Les Néandertaliens. Biologie et Cultures*. Paris, Comité des Travaux Historiques et Scientifiques (C.T.H.S.): 169-179.

MAZURIER A. & MACCHIARELLI R., 2005. Anterior deciduous dentition in Neanderthals: topographic variation in enamel thickness and inner structural morphology. *Bulletins et Mémoires de la Société d'Anthropologie de Paris*, **17**: 280 (abstract).

MENA C. A., 1971. Taurodontism. *Oral Surgery*, **22**: 812-823.

MOLNAR S., HILDEBOLT C., MOLNAR I. M., RADOVČIĆ J. & GRAVIER M., 1993. Hominid enamel thickness. I. The Krapina Neanderthals. *American Journal of Physical Anthropology*, **92** (2): 131-138.

OLEJNICZAK A. J. & GRINE F. E., 2005. High-resolution measurement of Neandertal tooth enamel thickness by micro-focal computed-tomography. *South African Journal of Science*, **101**: 219-220.

OLEJNICZAK A. J. & GRINE F. E., 2006. Assessment of the accuracy of dental enamel thickness measurements using microfocal X-ray computed tomography. *Anatomical Record A*, **288**: 263-275.

OLEJNICZAK A. J., SMITH T. M., FEENEY R. N. M., MACCHIARELLI R., MAZURIER A., BONDIOLI L., ROSAS A., FORTEA J., DE LA RASILLA M., GARCIA-TABERNERO A., RADOVČIĆ J., SKINNER M. M., TOUSSAINT M. & HUBLIN J.-J., 2008. Dental tissue proportions and enamel thickness in Neandertal and modern human molars. *Journal of Human Evolution*, **55** (1): 12-23.

RAMIREZ ROZZI F. V., 1996. Comment on the causes of thin enamel in Neandertals. *American Journal of Physical Anthropology*, **99** (4): 625-626.

RICHARDS M. P., PETTITT P. B., STINER M. C. & TRINKAUS E., 2001. Stable isotope evidence for increasing dietary breadth in the European mid-Upper Paleolithic. *Proceedings of the National Academy of Sciences USA*, **98**: 6528-6532.

ROUGIER H., CREVECOEUR I., FIERS E., HAUZEUR A., GERMONPRÉ M., MAUREILLE B. & SEMAL P., 2004. Collections de la Grotte de Spy: (re)découvertes et inventaire anthropologique. *Notae Praehistoricae*, **24**: 181-190.

SKINNER M. M., WOOD B. A., BOESCH C., OLEJNICZAK A. J., ROSAS A., SMITH T. M. & HUBLIN J.-J., 2008. Dental trait expression at the enamel-dentine junction of lower molars in extant and fossil hominoids. *Journal of Human Evolution*, **54**: 173-186.

SMITH P. & ZILBERMAN U., 1994. Thin enamel and other tooth components in Neanderthals and

other hominids. *American Journal of Physical Anthropology*, **95** (1): 85-87.

SMITH T. M., REID D. J., OLEJNICZAK A. J., BAILEY S., GLANTZ M., VIOLA B. & HUBLIN J.-J., 2011. Dental development and age at death of a Middle Paleolithic juvenile hominin from Obi-Rakhmat Grotto, Uzbekistan. *In*: S. CONDEMI & G.-C. WENIGER (ed.), *Continuity and discontinuity in the peopling of Europe. One hundred fifty years of Neanderthal study*. Dordrecht, Springer: 155-163.

SMITH T. M., TAFFOREAU P., REID D. J., GRÜN R., EGGINS S., BOUTAKIOUT M. & HUBLIN J.-J., 2007a. Earliest evidence of modern human life history in North African early *Homo sapiens*. *Proceedings of the National Academy of Sciences USA*, **104**: 6128-6133.

SMITH T. M., TAFFOREAU P., REID D. J., POUECH J., LAZZARI V., ZERMENO J. P., GUATELLI-STEINBERG D., OLEJNICZAK A. J., HOFFMAN A., RADOVČIĆ J., MAKAREMI M., TOUSSAINT M., STRINGER C. & HUBLIN J.-J., 2010. Dental evidence for ontogenic differences between modern humans and Neanderthals. *Proceedings of the National Academy of Sciences USA*, **107**: 20923-20928.

SMITH T. M., TOUSSAINT M., REID D. J., OLEJNICZAK A. J. & HUBLIN J.-J., 2007b. Rapid dental development in a Middle Paleolithic Belgian Neanderthal. *Proceedings of the National Academy of Sciences USA*, **104**: 20220-20225.

SPOOR C. F., ZONNEVELD F. & MACHO G., 1993. Linear measurements of cortical bone and dental enamel by computed tomography: applications and problems. *American Journal of Physical Anthropology*, **91** (4): 469-484.

SUWA G. & KONO R. T., 2005. A micro-CT based study of linear enamel thickness in the mesial cusp section of human molars: reevaluation of methodology and assessment of within-tooth, serial, and individual variation. *Anthropological Science*, **113**: 273-289.

TILLIER A.-M., ARENSBURG B. & DUDAY H., 1989. La mandibule et les dents du Néanderthalien de Kebara (Homo 2) Mont Carmel, Israël. *Paléorient*, **15**: 39-58.

TOUSSAINT M., OLEJNICZAK A. J., EL ZAATARI S., CATTELAIN P., FLAS D., LETOURNEUX C. & PIRSON S., 2010. The Neandertal lower right deciduous second molar from Trou de l'Abîme at Couvin, Belgium. *Journal of Human Evolution*, **58**: 56-67.

TRINKAUS E., 1983. *The Shanidar Neandertals.* New York, Academic Press: 502 p.

VALLOIS H. V., 1957. La dent humaine fossile du Lazaret. *Bulletin du Musée d'Anthropologie Préhistorique de Monaco*, **4**: 111-117.

WOLPOFF M. H., 1979. The Krapina Dental Remains. *American Journal of Physical Anthropology*, **50** (1): 67-114.

ZILBERMAN U., SKINNER M. & SMITH P., 1992. Tooth components of mandibular deciduous molars of *Homo sapiens sapiens* and *Homo sapiens neanderthalensis*: a radiographic study. *American Journal of Physical Anthropology*, **87** (3): 255-262.

ZILBERMAN U. & SMITH P., 1992. A comparison of tooth structure in Neanderthals and early *Homo sapiens sapiens*: a radiographic study. *Journal of Anatomy*, **180**: 387-393.

AUTHORS AFFILIATION

Priscilla BAYLE
Université de Bordeaux
PACEA, UMR 5199
Allée Geoffroy St Hilaire
CS 50023
33615 Pessac cedex
France
p.bayle@pacea.u-bordeaux1.fr

Roberto MACCHIARELLI
UMR 7194
Département de Préhistoire
du Muséum national d'Histoire naturelle
43, rue Buffon
75005 Paris
France
roberto.macchiarelli@mnhn.fr
and
Département Géosciences
Université de Poitiers
rue A. Turpain, bât. B8
86022 Poitiers
France
roberto.macchiarelli@univ-poitiers.fr